VNU Journal of Science: Mathematics - Physics
Journal homepage: https://js.vnu.edu.vn/MaP

Original Article

Optical Properties and Formation Mechanism of Gold Nanoparticles Fabricated by Sono-electrochemical Method

Nguyen Ngoc Dinh, Nguyen Duy Thien*

VNU University of Science, 334 Nguyen Trai, Thanh Xuan, Hanoi, Vietnam

Received 25th February 2025
Revised 3rd March 2025; Accepted 2nd April 2025

Abstract: Gold nanoparticles (Au NPs) were synthesized rapidly using the Sono-electrochemical method, using gold electrodes and hexadecyltrimethylammonium bromide (CTAB) as the reducing agent. This method offers high productivity, simple equipment, and is cost-effective. The resulting Au NPs exhibited sizes ranging from 20 to 60 nm. The UV-vis absorption spectra of the synthesized Au NPs show a peak due to surface plasmon resonance absorption at around 530–548 nm, corresponding to transverse electronic oscillation. The relationship between the size of the Au NPs and their absorption spectrum was also investigated. Additionally, the impact of current density, CTAB surfactant concentration, and acetone volume on the size and characteristic plasmon properties of the Au NPs was examined. The formation mechanism of the Au NPs was also discussed.

Keywords: Gold nanoparticles, UV-vis, Sono-electrochemical.

1. Introduction

Gold nanoparticles (Au NPs) have been receiving significant attention from scientists due to their unique properties and potential applications in various fields [1-4]. Au NPs exhibit fascinating optical properties due to a phenomenon called localized surface plasmon resonance (LSPR) [5, 6]. LSPR arises when the electrons in the nanoparticle collectively oscillate in response to incident light, leading to enhanced absorption and scattering of light. This property makes Au NPs valuable in applications such as surface-enhanced Raman spectroscopy (SERS) [7-9] and plasmonic solar cells [10, 11],... Au

---

* Corresponding author.
E-mail address: thiennd@hus.edu.vn

https//doi.org/10.25073/2588-1124/vnumap.5763

NPs are also considered biocompatible, meaning it is generally well-tolerated by living organisms. This characteristic makes Au NPs suitable for various biomedical applications [2-4, 12-15] such as drug delivery, targeted therapy, and bioimaging. They can also be functionalized with specific molecules to enhance their compatibility and targeting abilities. Au NPs exhibit unique catalytic properties, often referred to as heterogeneous catalysis. They can act as highly efficient catalysts for various chemical reactions, including oxidation, hydrogenation, and carbon-carbon bond formation. These catalytic properties have applications in areas such as green chemistry, energy conversion, and environmental remediation [16, 17].

Au NPs can be synthesized through various methods, including the reduction of the gold salt $HAuCl_4$, typically with commonly used reducing agents such as sodium borohydride [18], trisodium citrate [19], or X-ray irradiation [19]. Another approach involves the creation of Au NPs through Laser ablation of a gold target surface [20, 21]. However, a common drawback of these manufacturing methods is their reliance on expensive HAuCl4 raw materials or specialized equipment like laser systems and X-ray sources, which necessitate stringent management and large investment cost. In an effort to enhance the cost-efficiency of producing Au NPs, researchers have developed electrochemical and sono-electrochemical methods [22].

In this particular study, Au NPs were successfully synthesized directly from bulk gold using an innovative ultrasonic electrochemical method. Notably, this method incorporates several novel features. Instead of using a high-capacity specialized ultrasound machine, a smaller-capacity ultrasound machine was used, which significantly reduced the overall cost of the ultrasonic electrochemical system [23, 24]. Rather than using an ultrasonic buzzer as an electrode, a platinum (Pt) plate was used as the electrode. This design allows for the arbitrary adjustment of the electrode's surface area, leading to increased efficiency in Au NPs generation. Additionally, by using gold anodes instead of gold salts, this alternative helps reduce the cost of gold colloidal solutions compared to other methods [18, 19].

2. Experimental

2.1. Preparation of Au NPs

The synthesis was conducted within a simple two-electrode electrochemical cell, as shown in the schematic diagram in Figure 1a. The anode was a gold plate measuring 10 mm × 10 mm × 0.5 mm, while the cathode was a platinum plate with the same dimensions. The spacing between the electrodes was maintained at approximately 10 mm.

To synthesize Au NPs, a 20 ml electrolytic aqueous solution was used. The solution contained hexadecyltrimethylammonium bromide (CTAB) $[(C_{16}H_{33})N(CH_3)_3Br]$ as a surfactant, with a concentration ranging from 0.02 M to 0.08 M, with concentrations of 0.02 M, 0.04 M, 0.06 M, and 0.08 M, corresponding to pH values of 7.25, 6.91, 6.74, and 6.59, respectively. Additionally, an acetone volume ranging from 50 µl to 500 µl was added to the solution. The glass electrolytic cell containing the CTAB solution was then placed into an ultrasonic bath (ULTRASONIC LC 30H) with ultrasonic power is 100 w, ultrasonic cleaning frequency is 80 kHz. Throughout the preparation process, ultrasound irradiation was kept constant. The electrochemical process was carried out at a current density ranging from 6 mA/cm^2 to 22 mA/cm^2. The synthesis duration was 30 minutes, and the process was conducted at room temperature (25 ^oC). By combining electrochemical reduction and ultrasonic, the Au NPs were formed from the gold metal anode.

2.2. Characterization of the Synthesized Samples

The crystal structure of the Au NPs was analyzed using an X-ray diffractometer (SIEMENS D5005, Bruker, Germany) with Cu-$K_{\alpha1}$ (λ = 0.154056 nm) irradiation. The morphology of Au NPs was characterized using a transmission electron microscope (JEOL JEM 1010). The composition of the samples was determined by energy dispersive X-ray (EDX) spectrometer (EDS, OXFORD ISIS 300) attached to the JEOL-JSM 5410 LV scanning electron microscope. UV-vis absorption spectra of solutions containing dispersed Au NPs were collected with a Shimadzu UV 2450 PC spectrometer.

3. Results and Discussion

3.1. Structure of Au NPs

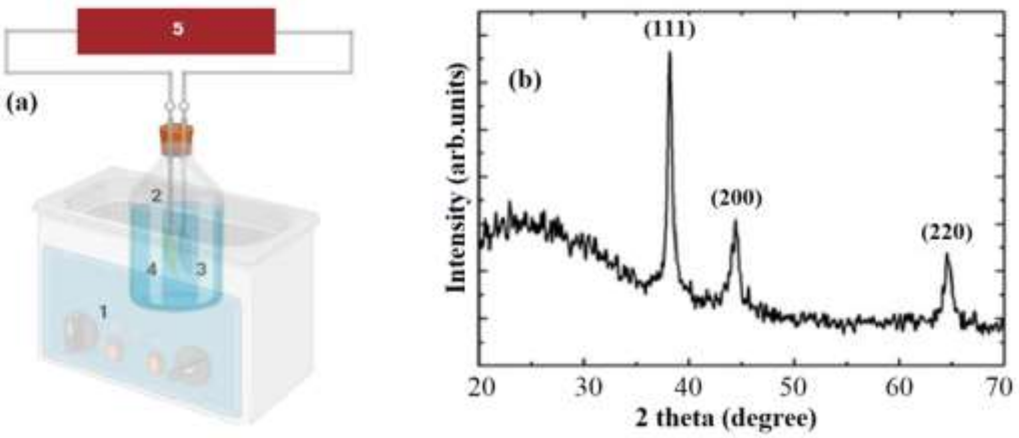

Figure 1. (a) The set-up for preparation of Au NPs by sono-electrochemical method. 1. Ultrasonic bath, 2. Glass vessel containing electrolyte, 3. Cathode (Pt), 4. Anode (Au), and 5. Power supply; (b) XRD patterns of Au NPs.

Figure 1b presents the X-ray diffraction (XRD) pattern of the Au NPs. The pattern exhibits three distinct diffraction peaks located at 38.15°, 44.35°, and 64.58°, which correspond to the diffraction planes of (111), (200), and (220), respectively. These results indicate that the Au NPs possess a face-centered cubic structure. The XRD analysis of the Au NPs revealed a lattice constant of a = 4.077 Å, which is found to be in excellent agreement with the standard diffraction patterns of cubic metallic gold (Pattern 7440-57-5). The close match between the determined lattice constant and the standard value provides strong evidence for the crystalline nature of the Au NPs and validates their structural properties. The average size of the Au NPs is estimated to be 14 nm using the Scherrer formula.

3.2. TEM Image of Au NPs in Correlation with UV-Vis Absorption Spectra

Figure 2 depicts the transmission electron microscopy (TEM) image of the fabricated Au NPs, along with the corresponding absorption spectrum. The results show that the absorption spectrum of the Au NPs exhibits characteristic plasmon peaks at different wavelengths depending on their size. Specifically, Au NPs with a size of approximately 20-25 nm show a plasmon peak at around 530 nm, while larger gold nanoparticles, ranging from 30-40 nm, exhibit a plasmon peak at approximately 545 nm.

According to Mie theory [6], a shift in the absorption peaks toward longer wavelengths signifies the presence of larger nanoparticles, while a shift toward shorter wavelengths indicates the presence of smaller nanoparticles. This phenomenon occurs due to the interaction of light with the nanoparticle's size and shape. When the nanoparticles are larger, they exhibit greater scattering and absorption of light, resulting in a shift toward longer wavelengths. Conversely, smaller nanoparticles scatter and absorb light differently, leading to a shift toward shorter wavelengths.

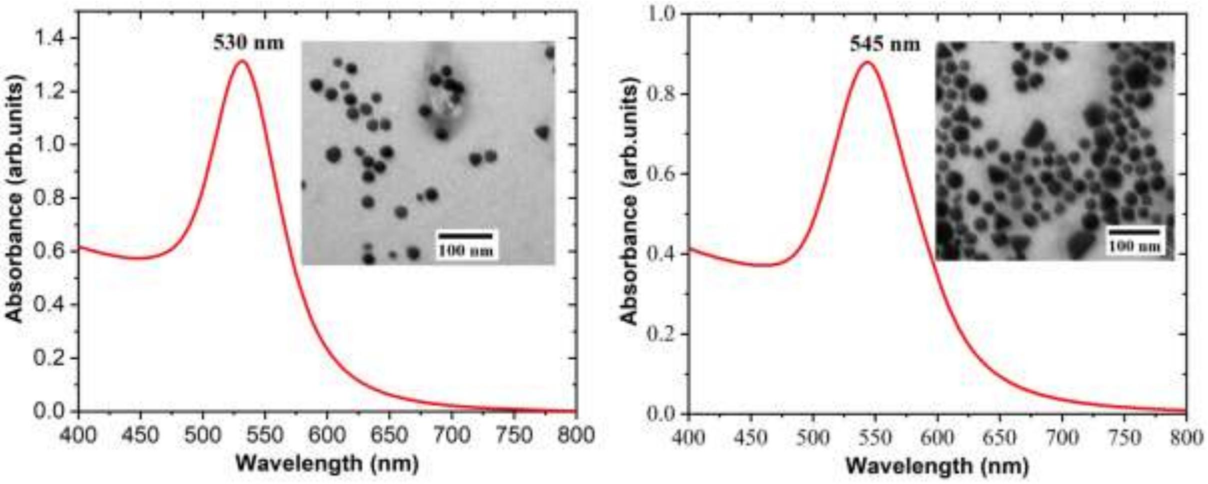

Figure 2. The TEM images and UV-Vis absorption spectrum of Au NPs.

3.3. *Effect of Preparation Conditions on Optical Properties of Au NPs*

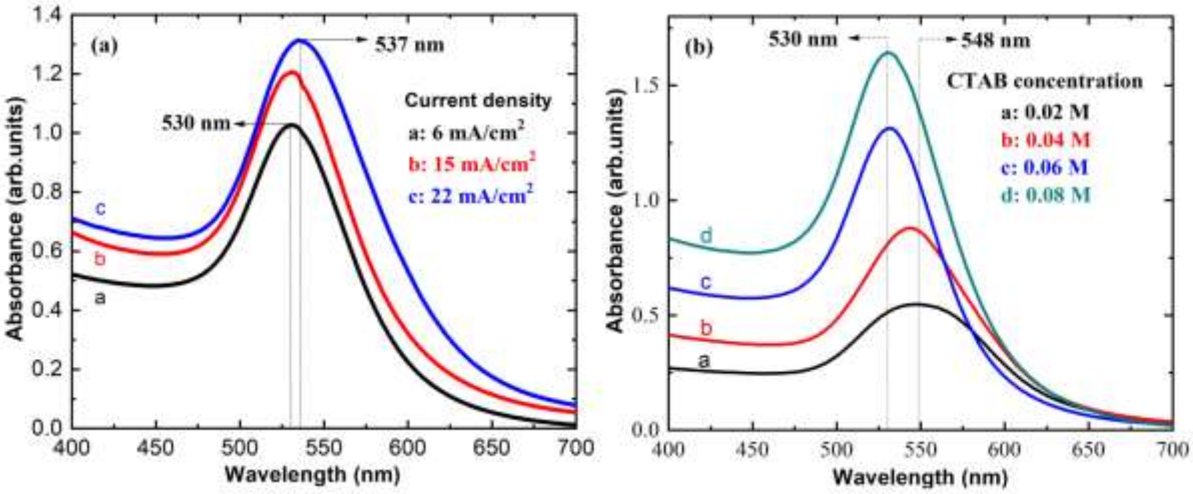

Figure 3. (a) The UV-Vis absorption spectrum of Au NPs produced under different current density of 6 mA/cm^2, 15 mA/cm^2, and 22 mA/cm^2; (b) The UV-Vis absorption spectra of the fabricated Au NPs by varying CTAB concentration.

In this study, we focused on the influence of current density, surfactant concentration, and acetone volume on the UV-Vis absorption spectrum of Au NPs. The UV-vis absorption spectrum of the synthesized Au NPs under different current densities (6 mA, 15 mA, and 22 mA) is presented in Figure 3a. Throughout the experiment, we maintained a constant electrode distance of 10 mm, an electrochemical time of 30 minutes, a CTAB concentration of 0.08 M, and an acetone volume of 50 µl. The results indicate that as the current density increases, the absorption peak corresponding to surface plasmon resonance in the UV-Vis absorption spectrum of Au NPs tends to shift toward longer wavelengths. Concurrently, the intensity of these absorption peaks also exhibits a significant increase.

Figure 3b displays the UV-Vis absorption spectrum of the fabricated Au NPs by varying the CTAB surfactant concentration (0.02 M, 0.04 M, 0.06 M, and 0.08 M). The experimental conditions, such as a current density of 6 mA, electrochemical time of 30 minutes, and acetone volume of 50 µl, were kept constant. The results indicate that when the CTAB concentration is low (0.02 M), the plasmon resonance absorption peak position of the Au NPs is significantly red-shifted (at 548 nm). However, as the CTAB concentration increases, this peak experiences a pronounced blue-shift toward shorter wavelengths. Concurrently, the intensity of the resonance absorption peak also shows an increase. CTAB, being a surfactant, plays a crucial role in this phenomenon. As the CTAB concentration increases, its ability to encapsulate the gold particles immediately after formation improves, preventing the agglomeration of nanoparticles and impeding the formation of larger Au NPs. Moreover, higher CTAB concentrations aid in stabilizing the dispersion of nanoparticles in the solution, ensuring their stable dispersion.

To investigate the effect of acetone volume, we maintained a constant electrolysis time of 30 minutes, an electrolytic current density of 6 mA, and a CTAB concentration of 0.08 M, while varying the acetone volume in the solution from 50 µl to 500 µl. Analyzing the UV-Vis absorption spectrum of the synthesized Au NPs as the acetone volume changed (Figure 4a), we observed that with increasing acetone volume, the surface plasmon resonance absorption peak position of the Au NPs exhibited a redshift toward longer wavelengths. However, beyond a certain threshold, the absorption peak began to shift in the opposite direction, showing a blue shift. This phenomenon is intriguing.

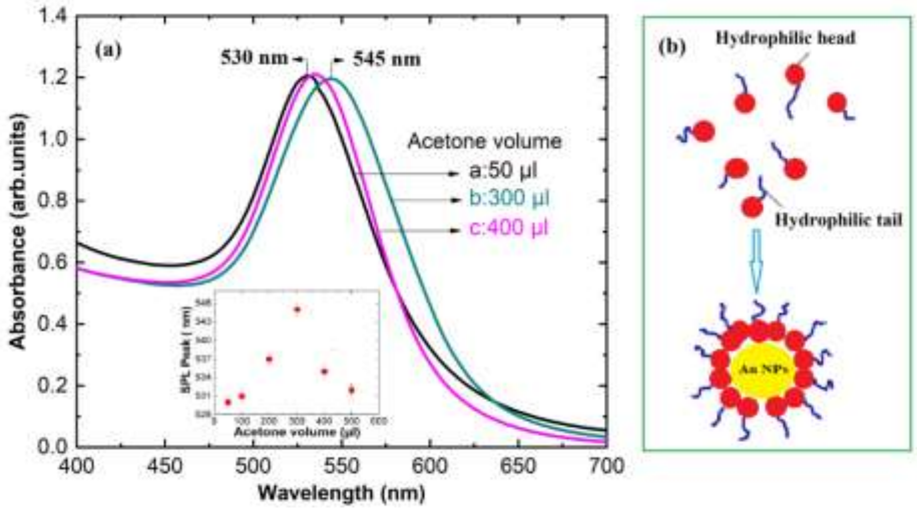

Figure 4. (a) UV-Vis absorption spectrum of fabricated Au NPs by varying acetone volume; (b) CTAB molecular model and Association of CTAB molecules with Au NPs.

The formation of gold nanoparticles is attributed to the interaction between the surfactant (CTAB) and the gold electrode. CTAB possesses a hydrophilic terminal structure connected to a hydrophobic chain. At relatively low concentrations, the hydrophobic ends of CTAB molecules are linked together by ionic bonds, resulting in a spherical shape, while the hydrophilic ends point outward, these structures are called micelles (Figure 4b) [25]. Under the action of the electric field, $AuBr_4^-$ is generated at the interface of anode . These ions are subsequently discharged from the surface of the anode and move toward the cathode. Upon reaching the cathode, these ions undergo adsorption onto the electrode's surface before undergoing a reduction process, eventually transforming into individual gold atoms.

$$AuBr_4^- + 2e^- = AuBr_2^- + 2Br.$$

$$AuBr_2^- - e^- = Au^o + 2Br^-.$$

Gold atoms combine to form atomic clusters that gradually grow into Au NPs and surrounded by micelles (Figure 4b). When subjected to ultrasound waves, the Au NPs formed on the cathode surface are dislodged from the electrode and dispersed into the solution.

In the experiment, acetone was used as a catalyst to expand the diameter of the micelles. Increasing the concentration of acetone resulted in an enlargement of the micelle diameter, allowing them to encapsulate larger clusters of gold atoms, thereby yielding larger gold nanoparticles. However, due to the limited bonding between the micelles, further increases in acetone concentration led to a disruption of the micelle structure and bond rupture. This disruption was exacerbated by acetone's strong evaporative activity, which altered the surface tension. Consequently, some acetone was released as the bonds broke, and the remaining acetone was only sufficient to form smaller micelles, resulting in the formation of smaller Au NPs (as observed in Figure 4(a)).

4. Conclusion

Au NPs have been successfully fabricated by Sono-electrochemical method. The X-ray diffraction (XRD) analysis confirms that the Au NPs possess a face-centered cubic structure with a lattice constant of 4.077 Å. Transmission electron microscopy (TEM) images reveal that the size of Au NPs can be controlled by adjusting experimental parameters such as current density, CTAB concentration, and acetone volume. UV-Vis absorption spectra indicate that increasing acetone concentration initially leads to larger nanoparticles, but further increases cause a redshift followed by a blue shift due to micelle disruption. CTAB plays a vital role in stabilizing the nanoparticles, preventing agglomeration, and promoting uniform size distribution. This study provides valuable insights into the fabrication of Au NPs and highlights the importance of controlling preparation conditions to achieve desired nanoparticle sizes and optical properties.

Acknowledgments

Authors acknowledge the financial support from the key project of Vietnam National University, Hanoi, No. QG 24.70.

References

[1] S. Eustis, M. A. El. Sayed, Why Gold Nanoparticles Are More Precious Than Pretty Gold: Noble Metal Surface Plasmon Resonance and its Enhancement of the Radiative and Nonradiative Properties of Nanocrystals of Different Shapes, Chem. Soc. Rev., Vol. 35, 2006, pp. 209-217, https://doi.org/10.1039/B514191E.

[2] S. J. Amina, B. Guo, A Review on the Synthesis and Functionalization of Gold Nanoparticles as a Drug Delivery Vehicle, Int J Nanomedicine., Vol. 15, 2020, pp. 9823-9857, https://doi.org/10.2147/IJN.S279094.

[3] I. Hammami, N. M. Alabdallah, A. A. Jomaa, M. Kamoun. Gold Nanoparticles: Synthesis Properties and Applications, Journal of King Saud University – Science, Vol. 33, No. 7, 2021, pp. 101560, https://doi.org/10.1016/j.jksus.2021.101560.

[4] K. Nejati, M. Dadashpour, T. Gharibi, H. Mellatyar, A. Akbarzadeh, Biomedical Applications of Functionalized Gold Nanoparticles: A Review, J Clust Sci., Vol. 33, 2022, pp. 1-16, https://doi.org/10.1007/s10876-020-01955-9.

[5] J. P. Juste, I. P. Santos, L. M. Marzán, P. Mulvaney, Gold Nanorods: Synthesis, Characterization and Applications, Coord. Chem. Rev., Vol. 249, No. 17-18, 2005, pp. 1870-1901, https://doi.org/10.1016/j.ccr.2005.01.030.

[6] A. Moores, F. Goettmann, The Plasmon Band in Noble Metal Nanoparticles: An Introduction to Theory and Applications, New J. Chem. Vol. 39, 2006, pp. 1121-1132, https://doi.org/10.1039/B604038C.

[7] P. G. Etchegoin, E. C. Le Ru, A Perspective on Single Molecule SERS: Current Status and Future Challenges, Phys. Chem. Chem. Phys.Vol. 10, No. 40, 2008, pp. 6079-6089, https://doi.org/10.1039/B809196J.

[8] S. Y. Ding, E. M. You, Z. Q. Tian, M. Moskovits, Electromagnetic Theories of Surface-Enhanced Raman Spectroscopy, Chem. Soc. Rev., Vol. 46, No. 13, 2017, pp. 4042-4076, https://doi.org/10.1039/C7CS00238F.

[9] N. D. Thien, T. H. Dang, S. C. Doanh, L. Q. Thao, N. Q. Hoa, N. N. Dinh, N. M. Hieu, L. V. Vu, A Study Onfabrication of SERS Substrates Base on Porous Si Nanostructures and Goldnanoparticles, J Mater Sci: Mater Electron. Vol. 34, 2023, pp. 94, https://doi.org/10.1007/s10854-022-09518-6.

[10] C. Nahm, H. Choi, J. Kim, D. R. Jung, C. Kim, J. Moon, B. Lee, B. Park, The Effects of 100 nm-diameter Au Nanoparticles on Dye-sensitized Solar Cells, Appl. Phys. Lett., Vol. 99, No. 25, 2011, pp. 253107, https://doi.org/10.1063/1.3671087.

[11] K. A. Dao, T. T. Nguyen, T. M. H. Nguyen, D. T. Nguyen, Comparison of Some Morphological and Absorption Properties of the Nanoparticles Au/TiO_2 Embedded Films Prepared By Different Technologies on the Substrates for Application in the Plasmonic Solar Cell, Adv. Nat. Sci.: Nanosci. Nanotechnol., Vol. 6, 2015, pp. 015018, https://doi.org/10.1088/2043-6262/6/1/015018.

[12] X. Huang, M. A. E. Sayed, Gold Nanoparticles: Optical Properties and Implementations in Cancer Diagnosis and Photothermal Therapy, J. Adv. Res., Vol. 1, No. 1, 2010, pp. 13-28, https://doi.org/10.1016/j.jare.2010.02.002.

[13] N. H. Luong, N. N. Long, L. V. Vu, N. H. Hai, T. N. Phan, T. V. A. Nguyen, Metallic Nanoparticles: Synthesis, Characterization and Application, Int. J. Nanotechnol., Vol. 8, No. 3-5, 2011, pp. 227-240, https://doi.org/10.1504/IJNT.2011.038201.

[14] K. Nejati, M. Dadashpour, T. Gharibi, H. Mellatyar and A. Akbarzadeh, Biomedical Applications of Functionalized Gold Nanoparticles: A Review. J Clust Sci. Vol. 33, 2022, pp. 1-16, https://doi.org/10.1007/s10876-020-01955-9.

[15] R. Stein, B. Friedrich, M. Mühlberger, N. Cebulla, E. Schreiber, R. Tietze, I. Cicha , C. Alexiou, S. Dutz, A. R Boccaccini, H. Unterwege, Synthesis and Characterization of Citrate-Stabilized Gold-Coated Superparamagnetic Iron Oxide Nanoparticles for Biomedical Applications, Molecules 2020, Vol. 25, No. 19, pp. 4425, https://doi.org/10.3390/molecules25194425.

[16] M. Perera, L. A. Wijenayaka, K. Siriwardana, D. Dahanayake, K. M. N. D. Silva, Gold Nanoparticle Decorated Titania for Sustainable Environmental Remediation: Green Synthesis, Enhanced Surface Adsorption and Synergistic Photocatalysis, RSC Adv., Vol. 10, 2020, pp. 29594-29602, https://doi.org/10.1039/D0RA05607C.

[17] L. X. Dien, Q. D. Truong, T. Murayama, H. D. Chinh, A. Taketoshi, I. Honma, M. Haruta, T. Ishida, Gold Nanoparticles Supported on Nb_2O_5 for Low-Temperature CO Oxidation and as Cathode Materials for Li-ion Batteries, Applied Catalysis A: General, Vol. 603, 2020, pp. 117747, https://doi.org/10.1016/j.apcata.2020.117747.

[18] L. I. M. Silva, A. P. Gramatges, D. G. Larrude, J. M. S. Almeida, R. Q. Aucélio, A. R. D. Silva, Gold Nanoparticles Produced Using $NaBH_4$ in Absence and in the Presence of One-Tail or Two-Tail Cationic Surfactants: Characteristics and Optical Responses Induced Aminoglycosides, Colloids and Surfaces A: Physicochemical and Engineering Aspects, Vol. 614, 2021, pp. 126174, https://doi.org/10.1016/j.colsurfa.2021.126174.

[19] N. N. Long, L. V. Vu, C. D. Kiem, S. C. Doanh, C. T. Nguyet, P. T. Hang, N. D. Thien, L. M. Quynh, Synthesis and Optical Properties of Colloidal Gold Nanoparticles, J. Phys.: Conf. Ser., Vol. 187, 2009, pp. 012026, https://doi.org/10.1088/1742-6596/187/1/012026.

[20] T. B. Nguyen, N. A. Nguyen, T. D. Tran, Production of SERS Substrates Using Ablated Copper Surfaces and Gold/Silver Nanoparticles Prepared by Laser Ablation in Liquids. J. Electron. Mater. Vol. 49, 2020, p p. 6232-6239, https://doi.org/10.1007/s11664-020-08373-7.

[21] T. B. Nguyen, N. A. Nguyen, G. L. Ngo, Simple and Rapid Method to Produce SERS Substrates Using Au Nanoparticles Prepared by Laser Ablation and DVD Template. J. Electron. Mater., Vol. 49, 2020, pp. 311-317, https://doi.org/10.1007/s11664-019-07754-x.

[22] D. W. Chou, C. J Huang, N. H. Liu, Synthesis of the Small and Uniform Gold Nanoparticles by Electrochemical Technique, J. Electrochem. Soc., Vol. 163, No. 10, 2016, pp. 603-607, https://doi.org/10.1149/2.0491610jes.

[23] J. A. F. García, J. S. Salzar, E. R. Cortes, G. F. Goya, V. C. Mata, J. A. P. Rojas, Effect of Ultrasonic Irradiation Power on Sonochemical Synthesis of Gold Nanoparticles, Ultrasonics-Sonochemistry, Vol. 70, 2021, pp. 105274, https://doi.org/10.1016/j.ultsonch.2020.105274.

[24] S. Yao, Y. Hu, G. Li, A One-Step Sonoelectrochemical Preparation Method of Pure Blue Fluorescent Carbon Nanoparticles Under A High Intensity Electric Field, Carbon, Vol. 66, 2014, pp. 77-83, https://doi.org/10.1016/j.carbon.2013.08.044.

[25] J. P. Juste, I. P. Santos, L. M. L. Marzán, P. Mulvaney, Gold Nanorods: Synthesis, Characterization and Applications, Coordination Chemistry Reviews, Vol. 249, 2005, pp. 1870-1901, https://doi.org/10.1016/j.ccr.2005.01.030.